Optimisation of a finite element mesh for plates subjected to in-plane patch loading

Ikhenazen, G., Saidani, M. & Kilardj, M.

Original citation & hyperlink:
Ikhenazen, G, Saidani, M & Kilardj, M 2019, 'Optimisation of a finite element mesh for plates subjected to in-plane patch loading', Journal of Mechanical Science and Technology, vol. (In-press), MEST-D-18-00205R2, pp. 1185-1193. https://dx.doi.org/10.1007/s12206-019-0218-0

DOI 10.1007/s12206-019-0218-0
ISSN 1738-494X
ESSN 1976-3824

Publisher: Springer

The final publication is available at Springer via http://dx.doi.org/ 10.1007/s12206-019-0218-0

Optimisation of a finite element mesh for plates subjected to in-plane patch loading

Ghania Ikhenazen[1*], Messaoud Saidani[2] and Madina Kilardj[1]

[1] *Faculty of Civil engineering, University of sciences and technology H. Boumediene, Algeria*

[2] *Faculty of Engineering and Computing, Coventry University, UK*

Abstract

In designing in-plane stressed thin plates, the loading condition where the uniform distributed edge forces are locally applied along one or more of the plate's boundaries are often encountered. This paper aims to investigate the optimal grid pattern that can be used in the analysis of the displacement and stress fields of a simply supported thin plate partially compressed. The plate modelling is created by means of an isoparametric rectangular element. This grid pattern is designed to satisfy good accuracy with low density. A convergence analysis is performed through different sets of meshes locally refined in a judicious way. For each focused field, the critical plate area is searched. Displacement and max stress values are recorded in the respective searched critical zone. Good results are obtained in seeking stress and displacement fields using respectively a small and a more expanded local refinement.

Keywords: Displacement curves; Finite element analysis; Optimal grid pattern; Partial compression; Stress; Thin plates

1. Introduction

The use of high strength plates in many civil, mechanical and aeronautical fields (large span roofs, tall silos, bridges and spacecraft, marine and offshore structures provide just some examples) is quite common in modern applications [1]. These important structural elements are generally subjected to several types of in-plane or lateral loadings that may be applied separately or in combination with each other. Among these different loadings, the in-plane loads are often larger than the other types from the magnitude point of view [2]. The in-plane stresses may be tensile, compressive or shear depending on the practical loading conditions stemming from the structure use.

Compressive stresses are the most common actions encountered in designing thin plates. Indeed, structural elements such as flanges must be capable to withstand partial compressive forces resulting from bending stress distribution, vertical stiffeners and thin webs should be able to undertake local compression field actions that derivate from shear loading [3]. Also, thin slender webs must be capable to resist heavy localised compressive stress due to patch loads which can result from wheel loads applied to flange of crane girder. Furthermore, in airframe a local compression is induced by an axial loading due to the action of the air loading on an aircraft wing; the aerodynamic heating of panels in supersonic aircraft can be approximated by non-uniform thermal compressive stresses as the temperature distribution is not uniform throughout the volume of the restrained plate [4].

Previous researches on finite element analyses of thin plates subjected to uniform in-plane loading have been carried out [2,5,6]. Although designers are always confronted to the issue of in-plane patch loadings, not enough studies have been carried out [7]. Rockey and Bagchi [8] presented finite element techniques for simply supported square plate under concentrated compression. Using finite element analysis, Gil-Martín et. al. [9] and Graciano et. al. [3] investigated the impact of in-plane patch loading respectively on the strength reduction in steel girders and on the behavior of unstiffened webs. Komur and Sonmez [10] and Prajapat et. al. [11] used the finite element method to investigate the elastic

buckling behavior of rectangular solid and perforated plates under compressive loading. The first authors found that the presence of circular holes did not decrease the elastic buckling load for both partial and concentrated loading and this was not the case with uniformly distributed loading. Meanwhile, in the second investigation the authors concluded that a plate with in-plane normal restraint at the unloaded boundaries behaves in the same manner as that subjected to bi-axial compressive loading.

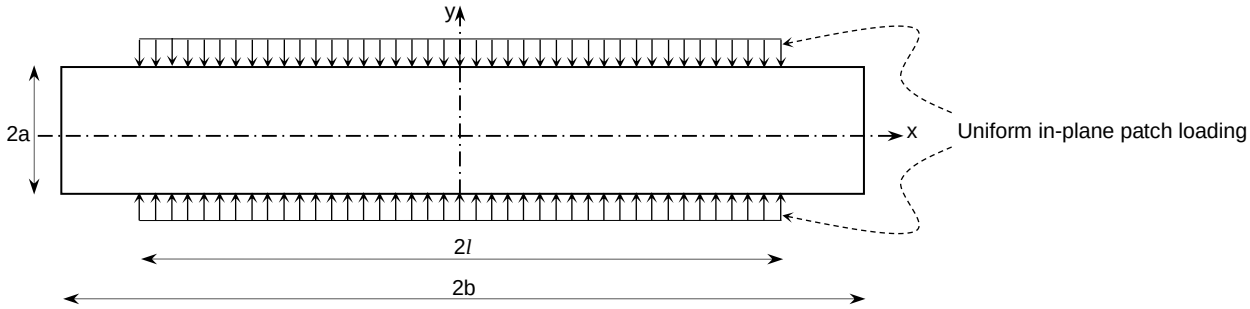

Fig. 1. Uniform compressive patch loaded plate, a: half width, b: half length, *l*: half loading length.

Before performing any finite element analysis of in-plane patch loaded plate such as stability, ultimate stress or natural frequencies analyses, a basic stress analysis is needed. In solving this quite not common problem where singularity is generated by a dramatic change of loading condition, additional difficulties are encountered. Indeed, the critical zone, area surrounding the point where the loading stops, has to be searched and then clearly defined. Also, because of the presence of this singularity, accurate solution requires particularly very tight refined grids with large computer time consumption. So, localized refinement in the critical zone associated with a low density grid may be very convenient in reaching this solution.

The present research deals with thin plates subjected to uniform compressive patch loading using the finite element method (see Fig. 1.). The authors aim to find the optimal grid, satisfying good accuracy with low density, which could be used in investigating displacement and stress fields. In this work

several convergence numerical tests has to be carried out. Different parameters such as the mesh pattern, the mesh density and the element shape have to be considered. In addition, the critical zone has to be defined. For this purpose, different sets of grids, regular with square elements and locally refined, have to be analysed. The tightest regular grid results are taken as reference and the critical zone is searched through various local refinements. The results of such research could be applied in seeking, for instance, the plate buckling shapes or the ultimate stress. In these issues, the displacement and the stress fields are respectively of particular interest. These results are also of practical importance when the solution in the immediate neighborhood of the singularity is of interest and when computations are performed for purposes of design certificate. This numerical analysis is performed with the commercial available software PAFEC-FE [12]. The obtained results are graphically summarised through displacements curves. Finally, some useful interpretations and a conclusion are given.

2. Plate modelling and problem formulation

2.1 Finite element version used

In finite element analysis, the approximation of the results depends on the number of degrees of freedom and on the way in which it is increased. In fact, there are three ways of increasing the number of degrees of freedom. First, the number of elements in the mesh is maintained and the number of nodes per element is increased (i.e. increase in the polynomial order). This process is called the 'P-version' [13,14]. Secondly, the polynomial order is maintained and an increase in the number of elements is made. This process leads to a decrease in the elements size and is called the 'H-version' where H is a representative of the element dimension. Clearly, a very large number of very small elements gives a virtually continuous structure, the behaviour of which is similar to a complete plate [15]. Finally, both the polynomial order and the number of elements in the mesh can be increased in the same time. This last process is called the 'H-P-version'. In the present work, the authors have used the 'H-version'.

2.2 Element type and capabilities

The present work deals with the stress analysis of thin plate with constant thickness *h.* The eight noded isoparametric quadrilateral element shown in Fig. 2 is used. The element is flat and carries loads in its own plane only. The element has in its own plane two degrees of freedom u_x and u_y which are two independent displacements. The assumptions are:

all bending and twisting effects acting out of plane of the element are ignored,

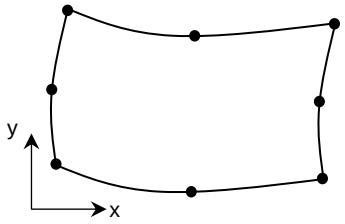

Fig. 2. Eight noded isoparametric quadrilateral element.

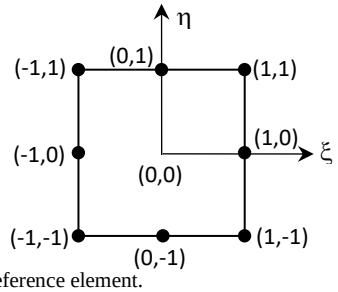

Fig. 3. Reference element.

– the gravity loads may give rise to loads perpendicular to the surface of the element. This load will have no effect on the element,

– the stresses do not vary through the thickness of the element.

2.3 Formulation of the plane stress analysis

In order to derive stiffness and other element matrices, the finite elements are transformed in a very simple shape in (ξ,η) domain [16,17,18]. This reference element (see Fig. 3) has four vertices and three

nodes along each of the element sides and the four vertices can lie anywhere in a plane. In practice, the eight nodes should form a shape that is quadrilateral with curved sides. To give a square of sides two units centred on the local coordinates axes ξ and η with vertex coordinates ±1 shown in Fig. 3, the following transformation is used:

$$\begin{Bmatrix} x \\ y \end{Bmatrix} = \begin{Bmatrix} \alpha_1 + \alpha_2\xi + \alpha_3\eta + \alpha_4\xi\eta + \alpha_5\xi^2 + \alpha_6\eta^2 + \alpha_7\xi^2\eta + \alpha_8\xi\eta^2 \\ \alpha_9 + \alpha_{10}\xi + \alpha_{11}\eta + \alpha_{12}\xi\eta + \alpha_{13}\xi^2 + \alpha_{14}\eta^2 + \alpha_{15}\xi^2\eta + \alpha_{16}\xi\eta^2 \end{Bmatrix} (1)$$

where *x* and *y* are the global coordinates. The transformation can conveniently be written in matrix form as:

$$\begin{Bmatrix} x \\ y \end{Bmatrix} = \begin{bmatrix} [P] & 0 \\ 0 & [P] \end{bmatrix} \begin{Bmatrix} \alpha_1 \\ to \\ \alpha_{16} \end{Bmatrix} \quad (2)$$

where the row matrix [*P*] of eight columns contains the polynomial terms in (ξ, η). The α_i are the arbitrarily constants. The number of terms in the polynomial [*P*] is equal to the number of nodes in the element.

As only the in-plane deformations are considered, the displacement field is completely defined by u_x et u_y which are the displacements in the *x* and *y* directions respectively. They are assumed to vary over the element in a manner corresponding exactly with the transformation assumption leading to the row matrix:

$$[U_x, U_y] = [P] \left[\begin{Bmatrix} \alpha_{17} \\ to \\ \alpha_{24} \end{Bmatrix}, \begin{Bmatrix} \alpha_{25} \\ to \\ \alpha_{32} \end{Bmatrix} \right] \quad (3)$$

where the α_i i=17 to 32 are the arbitrarily constants.

In order to derive the stiffness matrix, the strain energy and therefore the strains must be known. These latter are derived as follows:

$$\{\varepsilon\} = \begin{Bmatrix} \varepsilon_x \\ \varepsilon_y \\ \varepsilon_{xy} \end{Bmatrix} = \begin{Bmatrix} \partial u_x/\partial x \\ \partial u_y/\partial y \\ \partial u_x/\partial y + \partial u_y/\partial x \end{Bmatrix} \tag{4}$$

The stress vector is expressed as follows:

$$\{\sigma\} = \begin{Bmatrix} \sigma_x \\ \sigma_y \\ \tau_{xy} \end{Bmatrix} = [D]\{\varepsilon\} \text{ with } [D] = \frac{E}{1-\nu^2}\begin{bmatrix} 1 & \nu & 0 \\ \nu & 1 & 0 \\ 0 & 0 & (1-\nu)/2 \end{bmatrix} \tag{5}$$

where E is Young's modulus and ν is Poisson's ratio.

The strain energy stored in one element can be written in terms of the strain vector $\{\varepsilon\}$ and the stress vector $\{\sigma\}$ as follows:

$$U_e = \frac{1}{2}\iint_{element} \{\varepsilon\}^T\{\sigma\}\, h dx dy = \frac{1}{2}\{u_e\}^T[S_e]\{u_e\} \tag{6}$$

The matrix $[S_e]$ which is square and symmetric is known as the element stiffness matrix and the vector $\{u_e\}$ is the element displacement vector. The use of Castigliano's theorem yields to the generalised forces acting on the element in terms of displacements. This is done by differentiating the strain energy U_e with respect to displacements in the following way:

$$\frac{\partial U_e}{\partial\{u_e\}} = \{F_e\} = [S_e]\{u_e\} \tag{7}$$

Where $\{F_e\}$ is the generalised forces vector acting on the element.

The writing down of the equilibrium conditions between elements for the complete structure in terms of forces and then in terms of displacements yields a set of equations system for the displacements which can subsequently be solved. These equations can be written as follows:

$$\{F\} = [S]\{u\} \tag{8}$$

Where $\{F\}$ is the generalised forces vector acting on the whole structure and $[S]$ and $\{u\}$ are respectively the stiffness matrix and the unknown displacements vector for the whole structure. By knowing the nodal displacements on each element, the stresses can be derived by using equation (5) after substituting the strains obtained through equation (4).

3. Meshes Geometry

3.1 Assumed critical zone localisation

In order to find the more appropriate discretization for analysing the problem formulated in the present work, four different kinds of meshes: A, B, C and D are designed. These discretizations are considered in an effort to identify the assumed plate critical zone. The use of a typical pattern presenting a fine mesh in this zone and a coarser mesh elsewhere, would be justified and would save computation time without sacrificing accuracy.

At first sight, as there is a sudden change in the loading conditions at the plate boundary, it has been assumed that a zone of singularity could rise in the vicinity of the loading edge. Therefore, four points: P_1, P_2, P_3 and P_4 are judiciously chosen; they are positioned as follows (see Fig. 4)

– P_1 is the point where the distributed load stops,

– P_2 is at quarter width under P_1,

– P_3 and P_4 are located on the edge of the plate, respectively at the left and right hand side of P_1 and at the same distance from P_1.

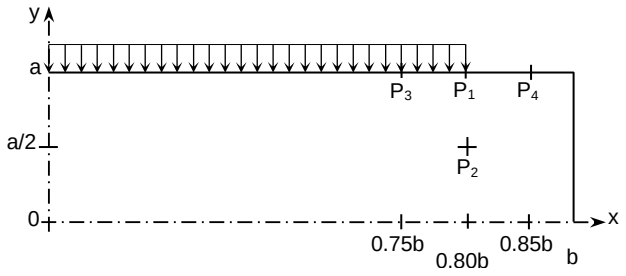

Fig. 4. Quarter of uniform compressive patch loaded plate with a/b=0.1, *l*/b=0.8 and a/*h*=100.

Because the plate and the loading are symmetrical, only a quarter of the plate is analysed. The displacements at P_i points are recorded. These displacements are u_x and u_y that are parallel respectively to the plate length and the plate width. In addition, the stress values all over the plate are derived and the stress values at the vicinity of P_1 are recorded.

3.2 Meshes Geometry description

To compare the different results, the A meshes are designed by using the same square element throughout the plate. This design gives regular grids [2,7,3,4] that are quite commonly used in finite element analysis. It should be noted that, in this type of discretization, the increase in the element number leads to a virtual continuous plate, the behaviour of which is similar to the real studied plate. The results stemming from the tightest of these first dicretizations, that do not distinguish any region in respect to another, will be taken as a reference in the present study. In the other hand, in the B, C and

D meshes, the area surrounding the loading stop point is assumed to be critical and thus is subdivided in relatively tight way [5,8,14]. Also, this area is assumed to be more and more extensive up to cover all the plate width. The discretization details are described in the following.

The A meshes depicted in Fig.5 constitute a set of three meshes that is obtained through uniform refinement by decreasing the size of the square element used. These mesh layouts are analysed in order to have a general idea about what it is happening over the plate without giving any particular attention to the singularities.

Using elements with trapezoidal shape, the B mesh is drawn by subdividing very tightly the direct surrounding of P_1, point where the loading stops. This model, in which the critical zone is assumed very tiny, is examined in order to see if the problem is particularly located at P_1. This mesh is depicted in Fig.6.

In the C meshes, the critical zone is assumed more extended than in the B mesh. Indeed, this critical zone extends up to the P_2, P_3 and P_4 points. By means of square elements, this zone is much more refined than the neighborhood of the loaded edge. Elsewhere, the mesh is relatively coarse as shown in Fig.7. A set of three C meshes are analysed.

Finally, a set of six discretizations noted D is analysed. In this last investigation, it is assumed that the critical zone goes beyond the area bounded by the P_i points and spreads all over the plate width, as it is shown in Fig.8. In this zone, the meshes are more and more refined by using different geometrical shapes of the quadrilateral element. Elsewhere, the meshes are uniformly discretized by rectangular elements in relatively coarse way.

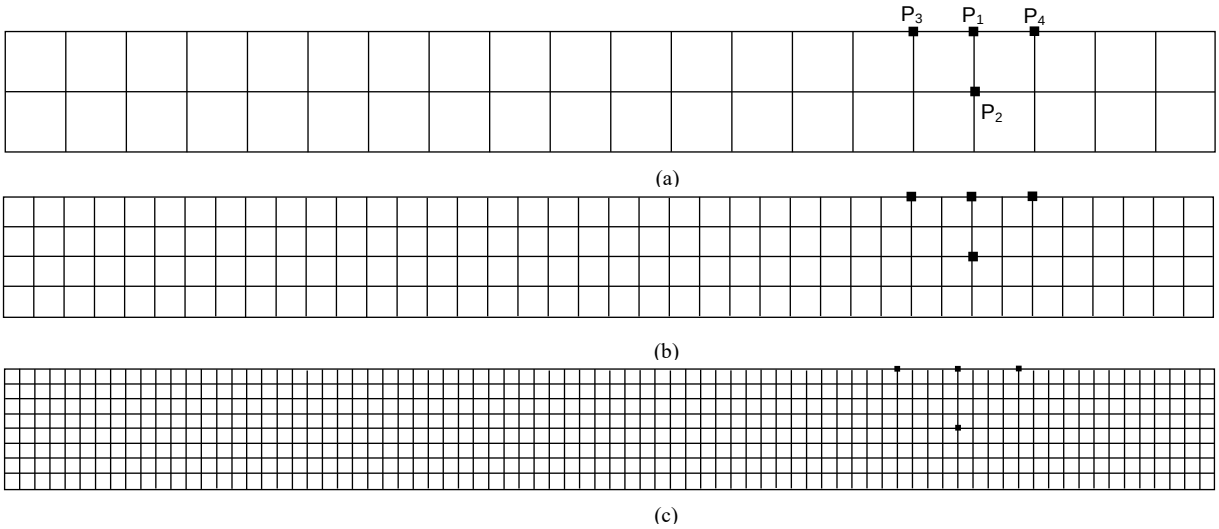

Fig. 5. Three discretizations of meshes A with: (a) 2x20 elements and 284 degrees of freedom, (b) 4x40 elements and 1 048 degrees of freedom, (c) 8x80 elements and 4 016 degrees of freedom.

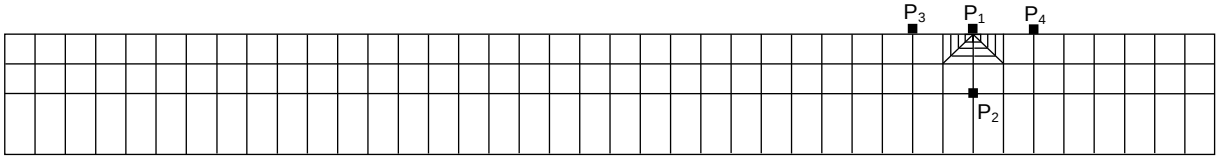

Fig. 6. Discretization of mesh B with 138 elements and 890 degrees of freedom.

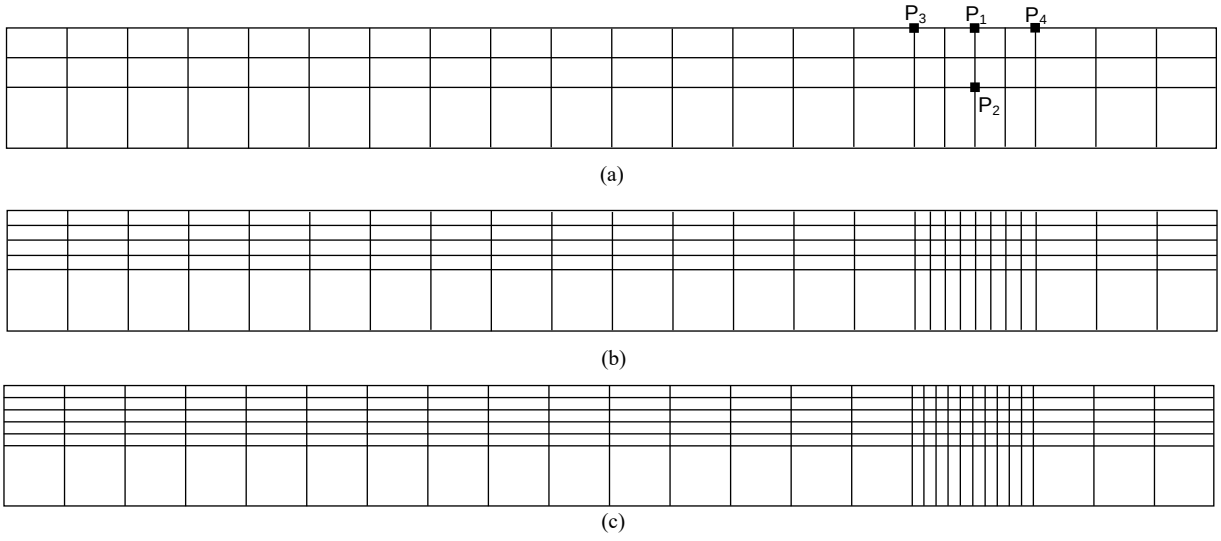

Fig. 7. Three discretizations of meshes C with: (a) 66 elements and 446 degrees of freedom, (b) 130 elements and 842 degrees of freedom, (c) 168 elements and 1 076 degrees of freedom.

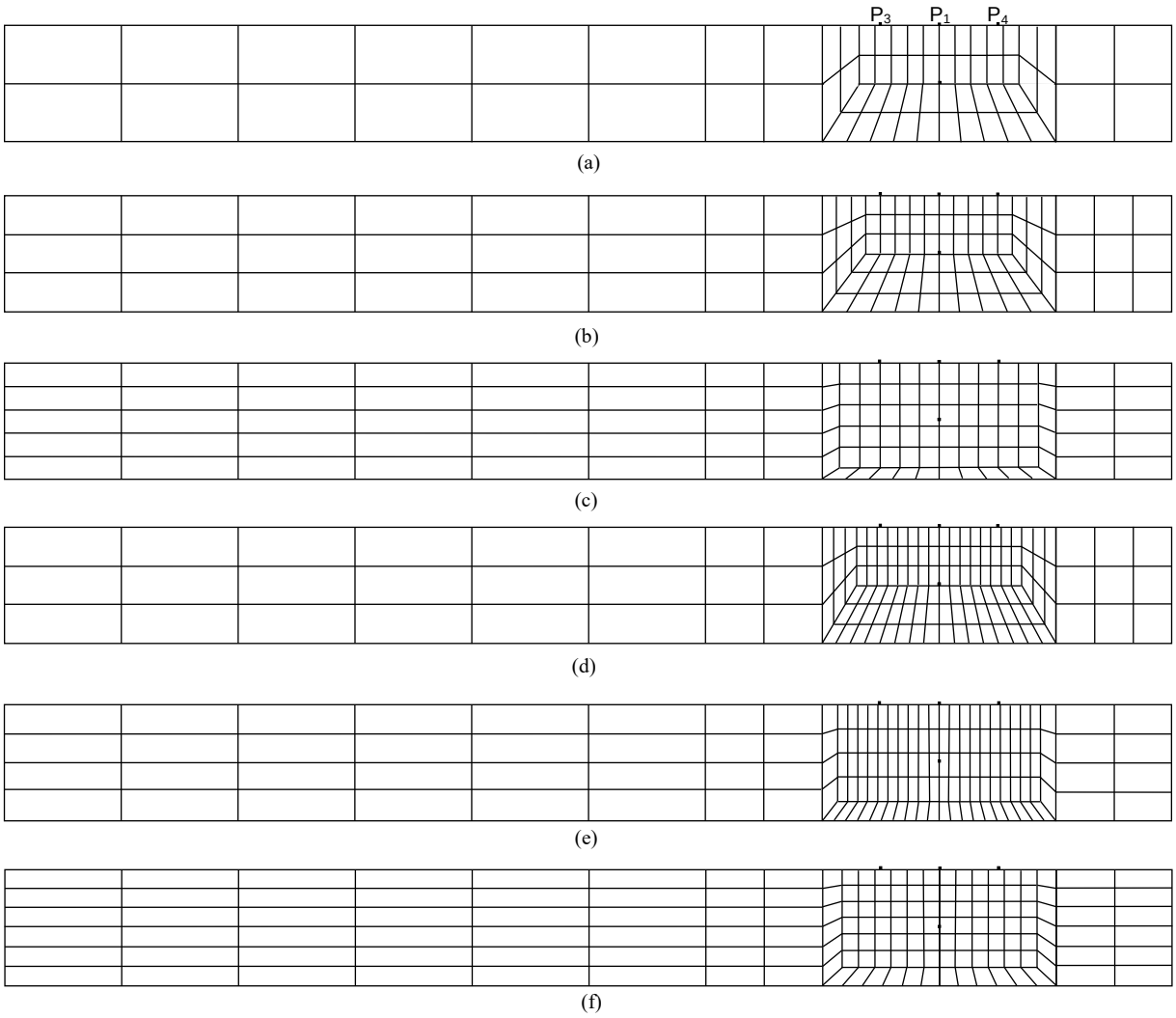

Fig. 8. Six discretizations of meshes D with: (a) 68 elements and 460 degrees of freedom, (b) 111 elements and 726 degrees of freedom, (c) 120 elements and 774 degrees of freedom, (d) 147 elements and 954 degrees of freedom, (e) 148 elements and 960 degrees of freedom, (f) 192 elements and 1 224 degrees of freedom.

4. Results presentation and interpretation

4.1 Introduction

As stated previously the aim of the present investigation is to find the more appropriate mesh pattern that it needs to be used in the partially compressed plate problems. The behaviour of such plates is examined through their displacement and stress fields. For this purpose, a thin simply supported plate along its central lines is analysed (see Figs. 1 and 4). The plate ratio is a/b=0.1 and the a/*h* ratio is equal to 100 where *h* is the plate thickness. The modulus of elasticity $E=209\times10^9 N/m^2$ and the Poisson's ratio

v is taken equal to 0.3. The 20×10^3KN/m compression is partially applied over a distance of $2l$ with a ratio l/b=0.8. In all meshes, the discretization is based on the rectangular isoparametric element described in section *2.2*. In the search of the optimal mesh, the thirteen meshes refined in different ways are treated. For each uniformly or locally refined grid, the displacements u_x and u_y at the four judiciously chosen points are recorded. In addition, for these meshes the maximum stresses at the direct vicinity of the loading stop point are recorded.

Table 1. Displacement u_x and u_y obtained from the different mesh discretizations.

mesh type	number of elements	number of degree of freedom (d.o.f)	log(d.o.f)	P_1 (0.80b,a) 10^{-6}m				P_2 (0.80b,0.50a) 10^{-6}m				P_3 (0.75b,a) 10^{-6}m				P_4 (0.85b,a) 10^{-6}m			
				u_x	Relative errors in %	u_y	Relative errors in %	u_x	Relative errors in %	u_y	Relative errors in %	u_x	Relative errors in %	u_y	Relative errors in %	u_x	Relative errors in %	u_y	Relative errors in %
A	40	284	2.45	20.062	0.87	-4.788	0.00	23.013	0.09	-2.395	0.00	20.240	0.09	-8.977	0.24	21.671	0.09	-0.581	0.34
	160	1048	3.02	19.946	0.29	-4.788	0.00	23.033	0.00	-2.395	0.00	20.223	0.00	-8.997	0.02	21.654	0.01	-0.581	0.34
	640	4016	3.60	19.888	0.00	-4.788	0.00	23.034	0.00	-2.395	0.00	20.222	0.00	-8.999	0.00	21.652	0.00	-0.579	0.00
B	132	890	2.94	19.836	0.26	-6.829	42.63	23.523	2.12	-3.684	53.82	20.896	3.33	-10.047	11.65	21.471	0.84	-1.074	85.49
C	66	446	2.65	19.946	0.29	-4.788	0.00	23.030	0.02	-2.395	0.00	20.227	0.02	-8.995	0.04	21.658	0.03	-0.583	0.69
	130	842	2.93	19.889	0.01	-4.788	0.00	23.032	0.01	-2.395	0.00	20.227	0.02	-8.997	0.02	21.658	0.03	-0.581	0.35
	168	1076	3.03	19.877	0.06	-4.788	0.00	23.032	0.01	-2.395	0.00	20.375	0.76	-8.552	4.97	21.800	0.68	-0.547	5.53
D	68	460	2.66	19.945	0.29	-4.788	0.00	23.031	0.01	-2.395	0.00	20.221	0.00	-9.001	0.02	21.652	0.00	-0.577	0.35
	111	726	2.86	19.904	0.08	-4.788	0.00	23.034	0.00	-2.395	0.00	20.222	0.00	-8.995	0.04	21.653	0.00	-0.579	0.00
	120	774	2.89	19.913	0.13	-4.788	0.00	23.114	0.35	-2.204	7.97	20.208	0.07	-9.106	1.19	21.753	0.47	-0.472	18.48
	147	954	2.98	19.927	0.20	-5.775	20.61	23.034	0.00	-2.395	0.00	20.201	0.10	-9.130	1.46	21.532	0.55	-0.717	23.83
	148	960	2.98	19.941	0.27	-4.788	0.00	-------	----	--------	----	20.207	0.07	-9.106	1.19	21.638	0.06	-0.592	2.24
	192	1224	3.09	19.900	0.06	-4.788	0.00	23.085	0.22	-2.276	4.97	20.213	0.04	-9.067	0.76	21.715	0.29	-0.511	11.74

4.2 Displacements field results

The displacements values are recorded for each point P_i i=1,2,3,4 located on the plate as described in section 3.1. Associated with corresponding relative errors, these displacements are shown in Table

1. The graphs in Figs. 9 to 12 represent the displacements u_x and u_y at respectively P_1, P_2, P_3 and P_4 points. The vertical axis shows the displacement u_x or u_y at 10^{-7} or 10^{-8} metre. The horizontal axis compares the logarithm of the meshes number of degrees of freedom. The three curves link up the numerical results reached for a given set of grids: A, C or D.

It can be seen from the above cited graphs that, as more elements are used in meshes A presenting only square elements, the displacements behave smoothly reaching up a constant value. As the meshes are more and more uniformly graded, they tend to give the characteristic of the exact solution called the smoothness [13]. In the present investigation, the tightest regular grid (third A grid) results are taken as reference. The second A mesh discretization is sufficient for achieving the searched displacements value with a maximum relative error of 0.35%.

The B mesh, which is unique and tightly refined only at P_1, gives values out of the range of the scale chosen for all the other results reaching up to 84.85% relative error as shown in Table 1. The results are far from the smoothness and therefore have not been represented on the graphs. Consequently, the tightened refinement that is localised only in a very reduced area of singularity is not the answer to the treated issue. This area needs to be wider. This fact will be confirmed by the other meshes results.

In Fig.9, the plotted results obtained from the set of meshes C are close to the smoothness in respect to u_x (with a maximum relative error of 0.29%) and they overlap the smoothness in respect to u_y. This tendency is also encountered in Fig. 10 representing the P_2 displacements field. On the other hand, in Figs. 11 and 12 representing respectively the P_3 and P_4 displacements fields, the C meshes give values which first follow the smoothness but then suddenly move away from this curve.

This displacement behaviour could be explained by the increase in the number of elements with large aspect ratio. But, as very good results have been achieved at P_1 and P_2 with the same mesh, this behaviour led to the assumption that the critical zone has to be widened and be spread beyond the points P_3 and P_4 covering all the width of the plate giving then the D grids. Meanwhile, the 130 elements C grid

gave the same relative error (0.35%) as the 160 elements uniform grid. In searching results improvement, i.e. minimum of number of elements in the mesh coupled with good relative error, the D grids are considered.

First, it can be noticed from Table 1 results that when using the D grids, 68 elements are sufficient for reaching the same relative error (0.35%) as this obtained with the 130 elements C grid or the 160 elements uniform A grid. This improvement in the result shows that the singularity area had effectively to be widened. Meanwhile, when the D meshes are strongly refined, the displacements exhibit oscillatory behaviour with large amplitudes. On some graphs the fluctuations curve is located above the smoothness, whereas in some others it is below or it cuts the smoothness as it is the case in Fig. 12. The achieved results show that the use of high density mesh not always yields a solution with good accuracy. Indeed, it appears clearly from these results that the association of the increase of the number of elements with very large aspect ratio and of those with no right angles led to considerable error.

According to the results reached through the different types of grid, it can be said that when displacement field is of interest and the desired degree of precision is such that no more than 0.35% relative error is acceptable, then it is possible to evaluate the displacements directly from the first D grid with 68 elements. A greater precision of 0.08% can be achieved by using the second D grid design with 111 elements.

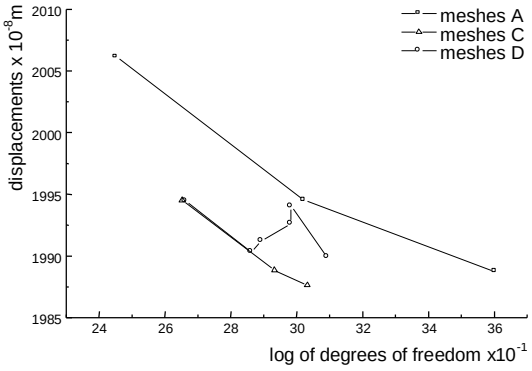

(a)

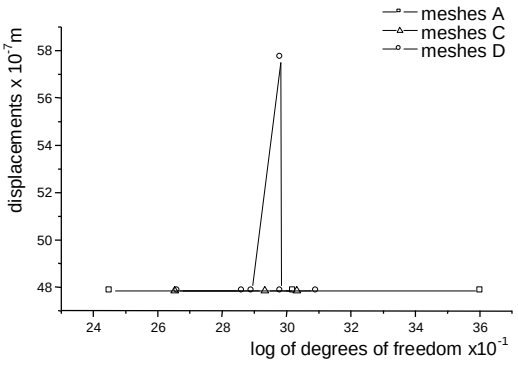

(b)

Fig. 9. Displacements at P_1: (a) in x direction, (b) in y direction.

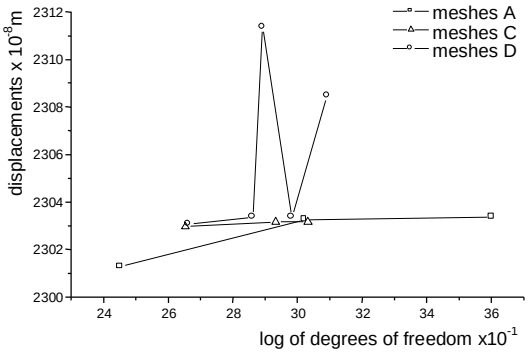

(a)

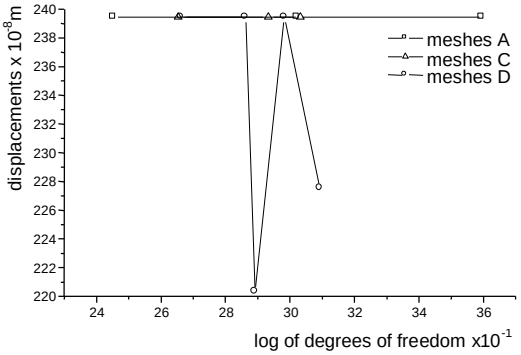

(b)

Fig. 10. Displacements at P_2: (a) in x direction, (b) in y direction.

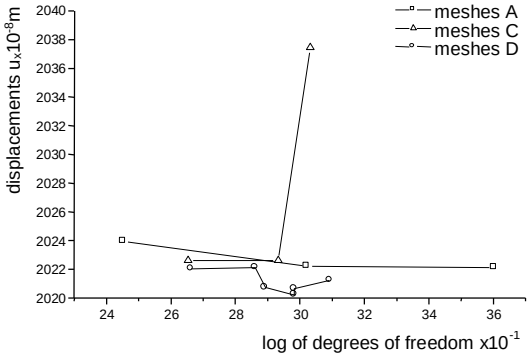

(a)

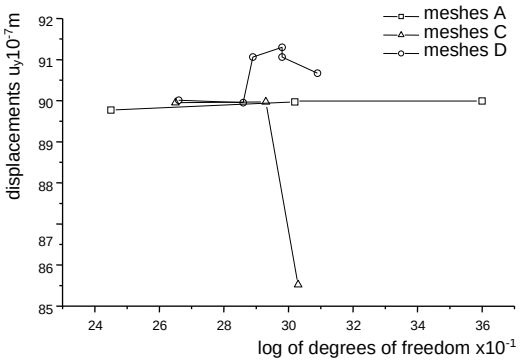

(b)

Fig. 11. Displacements at P_3: (a) in *x* direction, (b) in *y* direction.

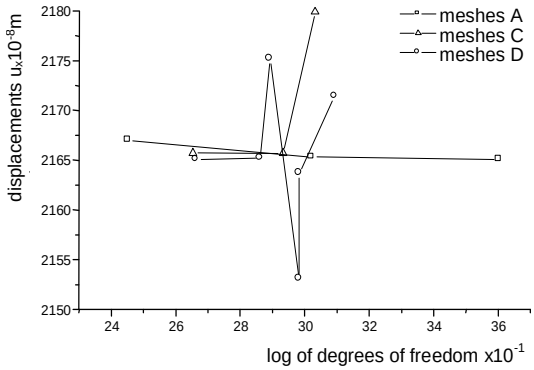

(a)

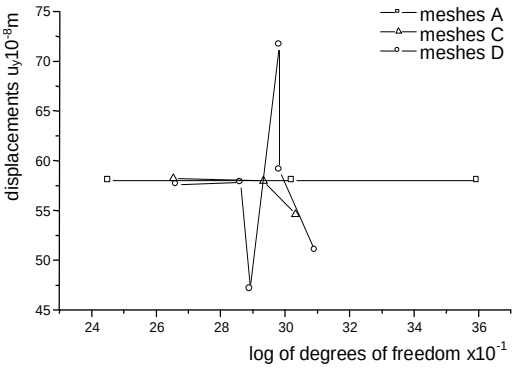

(b)

Fig. 12. Displacements at P_4: (a) in x direction, (b) in y direction.

4.3 Stress field results

H-convergence analysis has also been conducted in searching the optimal grid that leads to the stress field of a uniform patch compressed plate. This analysis was performed through the designed grids described in section 3.2.

As expected, the maximum stress values are located near the loading stop point P_1. These obtained results are depicted in Table 2 that reports, for the one B grid and the three sets of grids (A, C and D), the number of elements used in each discretization, the maximum stress recorded in the P_1 direct vicinity and the relative errors reached.

Table 2. Maximum stresses in the P_1 direct vicinity obtained from the different sets of grids.

Type of grids	Number of elements	Maximum stresses $/10^7[N.m^{-2}]$	Relative errors in %
A	2x20	-0.49	36.36
	4x40	-0.67	12.99
	8x80	-0.77	00.00
B	138	-1.08	40.26
C	66	-0.67	12.99
	130	-0.77	00.00
	168	-0.79	02.60
D	68	-0.69	10.39
	111	-0.74	03.90
	120	-0.73	05.19
	147	-0.72	06.49
	148	-0.71	07.79
	192	-0.75	02.60

It can be noticed from the figures that the third grid of meshes A, taken as reference, was not the model at which convergence has been smoothly reached.

Mesh B has overestimated the maximum stress value with a relative error of 40.26% and a fluctuating result was observed for all the other grids. As it was the case in seeking the displacement field, the

increase in the element number did not guarantee good accuracy and then the critical zone has to be judiciously defined.

With meshes D, as the number of elements was increased a relative error of 2.60% was obtained by using the 192 elements grid. This last result was reached by using only 168 elements with the third mesh C. Grids D seem to be the less appropriate in searching the stress field. On the other hand, the second mesh C gave the best numerical result as it reached 0% of relative error with only 130 elements in comparison with mesh of uniform grid A where the number of elements was five folded. Consequently, the second mesh C with a confined critical zone seems to be the most appropriate in evaluating the maximum stress in respect to the problem treated in the present work.

5. Conclusions

An H-convergence analysis has been performed on thin plate subjected to uniform compressive patch loading. The numerical tests have been conducted through different mesh patterns in order to select the optimal grid that can be used in seeking the displacement and the stress fields.

Very good results were obtained by means of locally refined mesh with 0% of relative error in seeking the stress field. Thus, refining finely a confined rectangular area, whose length is twice its width (width that is about one quarter of the considered plate), around the loading stop point was sufficient for reaching the wanted results.

On the other hand, when the displacement field was of particular interest, a mesh with more expanded locally refined area gave relatively good results. In respect to the tightest uniform grid taken as reference, only 10% and 17% of elements were needed to achieve respectively 0.35% and 0.08% maximum of relative error.

It has been shown that refinement in the singularity area gave good accuracy; the results indicate that proper mesh design is effective for controlling the error specially in the immediate vicinity of

the singular points. Also, it has been seen that the way in which the mesh is graded may lead to considerable error. So, when increasing the local refinement density, large aspect ratio and no right angles elements have to be avoided all over the plate and when this is observed, the desired results could be achieved efficiently.

Finally, it can be said that the designed sets of grids were find to be an effective analysis tool as the results obtained in this specific investigation could be applied in plate stability analyses such as buckling, in a strength checking or in seeking the required plate dimensions. Lastly, further research could involve undertaking numerical work in order to find the optimal grid pattern that could be adopted in other types of patch loadings with different boundaries conditions.

References

[1] M. Farshad, Design and analysis of shell structures, *Dordrecht: Kluwer Academic Publishers*, (1992).

[2] M.R. Khedmati, M.M Roshanali and Z.H.M.E Nouri, Strength of steel plates with both- sides randomly distributed with corrosion wastage under uniaxial compression, *Thin-walled structures*, 49 (2011) 325-42.

[3] C. Graciano and A. Ayestarán, Steel plate girder webs under combined patch loading, bending and shear, *Journal of Constructional Steel Research*, 80 (2013) 202-212.

[4] G. Ikhenazen, M. Saidani and A. Chelghoum, Finite element analysis of linear plates buckling under in-plane patch loading, *Journal of constructional steel research*, 66 (2010) 1112-1117.

[5] R. Brighenti, Buckling of cracked thin-plates under tension or compression, *Thin-walled structures*, 43 (2005) 209-24.

[6] R. Brighenti, Numerical buckling analysis of compressed or tensioned cracked thin plates, *Engineering structures*, 27 (2005) 265-76.

[7] M. Kilardj, G. Ikhenazen, T. Messager and T. Kanit, Linear and nonlinear buckling analysis of a locally stretched plate, *Journal of Mechanical Science and Technology*, 30 (8) (2016) 3607-3613.

[8] K. Rockey and D. Bagchi, Buckling of plate girder webs under partial edge loadings, *International Journal of Mechanics and Science*, 12 (1970) 61-76.

[9] L.M. Gil-Martín, B. Šćepanović, E. Hernández-Montes, M.A. Aschheim and D. Lučić, Eccentrically patch-loaded steel I-girders: The influence of patch load length on the ultimate strength, *Journal of Constructional Steel Research*, 66 (2010) 716-722.

[10] M.A. Komur and M. Sonmez, Elastic buckling behavior of rectangular plates with holes subjected to partial edge loading, *Journal of Constructional Steel Research*, 112 (2015) 54-60.

[11] K. Prajapat, S. Ray-Chaudhuri and A. Kumar, Effect of in-plane boundary conditions on elastic buckling behaviour of solid and perforated plates, *Thin Walled Structures*, 90 (2015) 171-182.

[12] Program for Automatic Finite Elements Calculations, Structural finite elements analysis software catering for: static, dynamic, non-linear, thermal analysis.

[13] B.A. Szabo, Estimation and control of error based on p-convergence, *Proc. Int. Conf. Accuracy Estimates and Adaptive Refinements in Finite Element Computations (ARFEC)*, (1984).

[14] J. Huang, N. Nguyen-Thanh , K. Zhou, . Extended isogeometric analysis based on Bézier extraction for the buckling analysis of Mindlin–Reissner plates, *Acta Mechanica*, 28 (2017), Issue 9, 3077–3093.

[15] O.C. Zienkiewicz, The finite element method in structural and continuum mechanics, *New York; McGraw-Hill*, (1967).

[16] O.C. Zienkiewicz, B.M. Irons, J. Ergatoudis, S. Ahmed and F.C. Scott. Isoparametric and associated element families for two and three-dimensional analysis. *Proc. course on finite element methods in stress analysis; Editions Holland I and Bell K. Trondheim, Tech. Univ*, (1969).

[17] O.C. Zienkiewicz and D.V. Philips. An automatic mesh generation scheme for plane and curved surfaces by isoparametric co-ordinates, *Int. J. Num. Meth. Engin*, 3 (1971) 519-28.

[18] B. Fraeijs de Veubeke, Bending and stretching of plates. *Proc. Conf. Matrix Meth. Struc. Mech. Wright Patterson Air Force Base, Dayton, Ohio*, (1965).